Total Proteome Analysis Identifies Migration Defects as a Major Pathogenetic Factor in Immunoglobulin Heavy Chain Variable Region (IGHV)-unmutated Chronic Lymphocytic Leukemia*⑤

Gina L. Eagle‡‖, Jianguo Zhuang‡‖**, Rosalind E. Jenkins§, Kathleen J. Till‡, Puthen V. Jithesh‡‡‡, Ke Lin¶, Gillian G. Johnson¶, Melanie Oates‡, Kevin Park§, Neil R. Kitteringham§, and Andrew R. Pettitt‡¶§§

The mutational status of the immunoglobulin heavy chain variable region defines two clinically distinct forms of chronic lymphocytic leukemia (CLL) known as mutated (M-CLL) and unmutated (UM-CLL). To elucidate the molecular mechanisms underlying the adverse clinical outcome associated with UM-CLL, total proteomes from nine UM-CLL and nine M-CLL samples were analyzed by isobaric tags for relative and absolute quantification (iTRAQ)-based mass spectrometry. Based on the expression of 3521 identified proteins, principal component analysis separated CLL samples into two groups corresponding to immunoglobulin heavy chain variable region mutational status. Computational analysis showed that 43 cell migration/adhesion pathways were significantly enriched by 39 differentially expressed proteins, 35 of which were expressed at significantly lower levels in UM-CLL samples. Furthermore, UM-CLL cells underexpressed proteins associated with cytoskeletal remodeling and overexpressed proteins associated with transcriptional and translational activity. Taken together, our findings indicate that UM-CLL cells are less migratory and more adhesive than M-CLL cells, resulting in their retention in lymph nodes, where they are exposed to proliferative stimuli. In keeping with this hypothesis, analysis of an extended cohort of 120 CLL patients revealed a strong and specific association between UM-CLL and lymphadenopathy. Our study illustrates the potential of total proteome analysis to elucidate pathogenetic mechanisms in cancer. *Molecular & Cellular Proteomics 14: 10.1074/mcp.M114.044479, 933–945, 2015.*

Chronic lymphocytic leukemia (CLL)[1] is the most common adult leukemia in Western countries. It is characterized by the clonal expansion of antigen-experienced B cells with a distinctive immunophenotype (1, 2). The disease runs a highly variable clinical course, with some patients surviving for decades without treatment and others dying from drug-resistant disease within a year of presentation (3).

Many biological variables have been identified in CLL that correlate with clinical outcome. Among these variables, the somatic mutational status of the immunoglobulin heavy chain variable region (IGHV) gene expressed by the malignant clone has a unique biological importance as it is the only prognostic biomarker that is fixed at the initiation of clonal expansion, inherited by the entire malignant clone, and stable over time (4–6). Furthermore, because somatic hypermutation is tightly regulated during B cell development, IGHV mutational status provides insight into the clonogenic cell of origin in CLL. Specifically, cases of CLL with mutated IGHV genes (M-CLL) are thought to arise from a memory B cell that has encountered a T cell-dependent antigen, whereas those with unmutated IGHV genes (UM-CLL) are thought to arise from a B cell that has reacted to a T-independent antigen (7). Importantly,

[1] The abbreviations used are: CLL, chronic lymphocytic leukemia; M-CLL, IGHV-mutated CLL; UM-CLL, IGHV-unmutated CLL; IGHV, immunoglobulin heavy chain variable region; ACN, acetonitrile; MS, mass spectrometry; iTRAQ, isobaric tags for relative and absolute quantification; PANTHER, Protein Analysis Through Evolutionary Relationships; MNDA, myeloid cell nuclear differentiation antigen; PCA, principal component analysis.

IGHV status is a strong and independent predictor of outcome in CLL, with M-CLL being associated with a favorable outcome and UM-CLL being associated with early disease progression and shorter survival (4–6).

Gene expression profiling studies have shown that, irrespective of their IGHV mutational status, CLL cells have an mRNA signature similar to that of memory B cells (8, 9). Although supervised clustering has shown that a number of genes are differentially expressed in M-CLL and UM-CLL (8, 9), the molecular mechanisms responsible for the more aggressive clinical course of UM-CLL remain incompletely understood. This may reflect the inability of mRNA profiling to detect differences in protein expression due to post-transcriptional regulation (10).

The advent of two-dimensional gel electrophoresis and mass spectrometry (MS) in the mid-1990s represented a technological breakthrough in profiling gene expression at the protein level (11, 12). Application of this technique to the question of how M-CLL and UM-CLL differ from one another has revealed a limited number of differentially expressed proteins (the details of which are provided in supplemental Table S1) (13–18). However, these studies have failed to provide a convincing explanation for the adverse clinical outcome associated with UM-CLL.

The ability of two-dimensional gel electrophoresis and MS to detect differences in protein expression is limited by the fact that they provide only limited coverage of the proteome and suffer from poor reproducibility (19). Recently, more powerful gel-free techniques for proteomic analysis have been developed, such as isobaric tags for relative and absolute quantification (iTRAQ)-based MS. Here, we describe the application of iTRAQ-based MS to analyze the total proteome of nine M-CLL and nine UM-CLL samples. This approach has enabled us to generate the largest quantity of proteomic information for CLL to date and, in particular, to directly compare the functions of differentially expressed proteins between UM-CLL and M-CLL cells through a systems biology approach. Our findings strongly support the idea that M-CLL and UM-CLL are biologically distinct and suggest that the adverse outcome associated with UM-CLL reflects the propensity of malignant cells to be retained in lymph nodes, where they are induced to proliferate. In keeping with this observation, we found a strong and specific association between UM-CLL and lymphadenopathy.

EXPERIMENTAL PROCEDURES

Sample Selection—All samples used for this study were obtained with informed consent and with the approval of the North West 2 Research Ethics Committee–Liverpool Central. Samples were characterized for IGHV mutational status as described below. Because the extent of IGHV mutation in CLL varies continuously from 0 to >10%, a cutoff value of 2% was applied to distinguish M-CLL from UM-CLL. This cutoff was used in the original studies describing the prognostic importance of IGHV mutation (4, 5) and continues to be applied (20). Nine cases were selected to represent extremely low levels of IGHV mutation, and nine were selected to represent extremely high levels. Care was taken to ensure that other biological variables of prognostic significance were evenly balanced between the two groups. The clinical features of the 18 CLL samples used for this study are shown in Table 1.

Preparation of CLL Samples—Venous blood was drawn from CLL patients into tubes containing sodium heparin at a final concentration of 10 units/1 ml of blood. Mononuclear cells were isolated by centrifugation of blood over Lymphoprep (Axis-Shield PoC AS, Oslo, Norway) within 4 h of sampling and stored at $-150\,°C$ within 2 h of separation. Analysis for recurrent chromosomal abnormalities was performed as described previously (21). All mononuclear cell samples used in the study contained >90% $CD19^+$ cells.

IGHV Mutational Analysis—Total RNA was extracted from CLL cells using an RNeasy mini kit (Qiagen, Crawley, UK). 1 μg of RNA was reverse-transcribed with Moloney murine leukemia virus reverse transcriptase (Promega, Southampton, UK) and an oligo(dT)$_{15}$ primer. Aliquots of the resulting cDNAs were used to identify clonally expressed IGHV in six PCRs, each with one of the six 5′-leader primers (22) and three mixed 3′-primers specific for the immunoglobulin heavy chain isotypes α, γ, and μ (23), respectively. The 50 microliter PCR containing 20 pmol of each primer, 1.5 mM $MgCl_2$, 100 μM each dNTP, and 2.5 units of *Taq* polymerase (Promega) was performed for 30 cycles by using a touch-down protocol, with the annealing temperature reducing from 63 to 57 °C over the first 12 cycles. The PCR products were visualized following electrophoresis. The amplified clonal IGHV gene was purified using the Wizard SV Gel and PCR Clean-up system (Promega), followed by Sanger sequencing from both directions with the same primers used in PCR. The IGHV gene usage and extent of somatic hypermutation were determined by comparison to the nearest germ line counterpart sequence in the international ImMunoGeneTics information system with IMGT/V-QUEST.

Protein Extraction and iTRAQ Labeling—Protein was extracted from CLL cells by sonication on ice in 500 mM triethylammonium bicarbonate with 0.1% SDS. Protein concentrations were determined using Bradford assay reagent (Sigma-Aldrich, Gillingham, UK). Labeling with iTRAQ reagents was then carried out according to the AB SCIEX (Framingham, MA) protocol for an 8plex procedure as described previously (24), but with the following modifications. Briefly, 100 μg of protein from each sample was reduced with tris(2-carboxyethyl)phosphine hydrochloride and capped with methyl methanethiosulfate before overnight digestion with trypsin (Promega). Peptides were then labeled with isobaric tags, pooled, diluted to 5 ml with 10 mM potassium dihydrogen phosphate and 25% acetonitrile (ACN), and acidified to pH <3 with phosphoric acid.

Sample Prefractionation and Desalting—Samples were fractionated on a PolySULFOETHYL A strong cation-exchange column (200 × 4.6 mm, 5 μm, 300 Å; Poly LC, Columbia, MD) at 1 ml/min using a gradient from 10 mM potassium dihydrogen phosphate and 25% (w/v) ACN to 0.5 M potassium chloride, 10 mM potassium dihydrogen phosphate, and 25% (w/w/v) ACN over 75 min. Fractions of 2 ml were collected and dried by centrifugation under vacuum (SpeedVac, Eppendorf UK, Stevenage, UK). Fractions were reconstituted in 1 ml of 0.1% trifluoroacetic acid and desalted using an mRP high-recovery protein column (4.6 × 50 mm; Agilent, Berkshire UK) on a VISION workstation (Applied Biosystems/Life Technologies, Paisley, UK) prior to MS analysis.

MS Analysis of iTRAQ Samples—Desalted fractions were reconstituted in 40 microliters of 0.1% formic acid, and 5 microliter aliquots were delivered into a TripleTOF 5600 system (AB SCIEX) via an Eksigent NanoUltra cHiPLC system (AB SCIEX) mounted with a microfluidic trap and an analytical column (15 cm × 75 micrometer) packed with ChromXP C_{18}-CL (3 μm). A NanoSpray III source was fitted with a 10 μm inner diameter PicoTip emitter (New Objective,

TABLE I
Clinical features of the 18 CLL samples subjected to iTRAQ-MS

Clinical feature	M-CLL (*n* = 9)	UM-CLL (*n* = 9)	*p*
Age at diagnosis (median), years	67	70	0.694
Gender (males/females)	3/6	6/3	0.347
Prior therapy (treated/untreated)[a]	3/6	2/7	0.620
Leukocyte count at time of sampling (median), $\times 10^9$/liter	78.4	135.8	0.423
High-risk chromosomal abnormalities (17p− and/or 11q−; yes/no)[b]	2/7	2/7	1.000
IGHV (median), %[c]	7.48	0.34	0.00004

The statistical significance of the difference (*p* values) between the two groups was determined using a two-tailed Mann-Whitney *U* test for parametric data and Fisher's exact test for nonparametric data, respectively.

[a] Prior therapy consisted of various combinations of glucocorticoid, chlorambucil, fludarabine, or fludarabine plus cyclophosphamide.

[b] CLL samples were tested by interphase fluorescence *in situ* hybridization for del17p13 (17p−), del11q23 (11q−), trisomy 12 (12+), and del13q14 (13q−). 17p and 11q− are regarded as high-risk chromosomal abnormalities.

[c] IGHV refers to somatic mutation in the IGHV gene of CLL cells compared with the gene sequence of the nearest germ line, where <2% was classed as UM-CLL and ≥2% was classed as M-CLL.

Woburn, MA). The trap column was washed with 2% ACN and 0.1% formic acid for 10 min at 2 microliter/min before switching in-line with the analytical column. A gradient of 2–50% ACN and 0.1% (v/v) formic acid over 90 min was applied to the column at a flow rate of 300 nl/min. Spectra were acquired automatically in positive ion mode using information-dependent acquisition powered by Analyst TF 1.5.1 software (AB SCIEX). Up to 25 MS/MS spectra were acquired per cycle (10 Hz) using a threshold of 100 counts/s and with dynamic exclusion for 12 s. The rolling collision energy was increased automatically by selecting the iTRAQ check box in Analyst and manually by increasing the collision energy intercepts by 5.

iTRAQ Data Analysis—Data were searched using ProteinPilot 4.2 and the Paragon Algorithm (AB SCIEX) against the Swiss-Prot database (2013-2, 40,646 human entries), with methyl methanethiosulfate as a fixed modification of cysteine residues and biological modifications allowed. Mass tolerance for precursor and fragment ions was 10 ppm. The data were also searched against a reversed decoy database, and only proteins lying within a 1% global false discovery rate were taken forward for analysis (25, 26). Each 8plex iTRAQ-MS experiment consisted of three M-CLL samples, three UM-CLL samples, a replicate sample, and a common reference sample consisting of a pool of all 18 samples. Quantitation of proteins was relative to the common pooled sample present in each iTRAQ-MS experiment. iTRAQ data for proteins identified by two or more peptides with at least 90% confidence of correct sequence assignment or by a single peptide with at least 99% confidence were log2-transformed, batch-corrected using the Batch Remover tool in the Partek Genomics Suite (version 6.3, Partek, St. Louis, MO), and included in subsequent analyses. The MS proteomic data have been deposited in the ProteomeXchange Consortium (27) via the PRIDE partner repository with the data set identifiers PXD001512, PXD001515, and PXD001516.

Principal Component Analysis (PCA)—PCA was performed using the Partek Genomics Suite (version 6.3) to assess variance across the sample set. A correlation method, which adjusts the data to be standardized to a mean of zero and an S.D. of 1, was used for dispersion matrix. Eigenvector scaling was performed orthogonal to the original variables and scaled to unity.

Statistical Analysis—Statistical significance of the difference in the levels of expression of proteins between UM-CLL and M-CLL samples was determined using Student's *t* test (two-tailed and unpaired), and proteins whose levels of expression were significantly different (*p* < 0.05) were included in subsequent analyses. Statistical analysis was conducted using the R computational environment (28).

Heat Maps—To detect outliers, hierarchical agglomerative clustering with complete linkage and Euclidean distance measure was employed on the selected data, and heat maps were drawn using the heatmap.2 package in R (28).

Computational Functional Analysis—Proteins found to have significantly higher or lower levels of expression in UM-CLL samples by iTRAQ-MS (*p* < 0.05) were subjected to computational functional analysis. Proteins were functionally classified using the Protein Analysis Through Evolutionary Relationships (PANTHER) classification system. Pathway analysis was conducted using the GeneGo pathway maps in the MetaCore database (version 6.14, build 61508; Thomson Reuters, New York, NY). The Pathway Maps tool was used to enrich for pathways, and *p* values were calculated based on a hypergeometric distribution, with the default database used as the background. Significant pathway enrichment was defined as a false discovery rate-corrected *p* < 0.05.

Western Blotting—Proteins were separated on an SDS-polyacrylamide gel and transferred to Immobilon-P polyvinylidene difluoride membranes (Millipore, Bedford, MA), which were probed with rat monoclonal MNDA (myeloid cell nuclear differentiation antigen), rabbit monoclonal LEF-1 (lymphoid enhancer-binding factor 1), and rabbit polyclonal TCL-1 (T cell leukemia/lymphoma 1) antibodies (all from Cell Signaling Technologies, New England Biolabs, Herts, UK), and mouse monoclonal β-actin antibody (Sigma-Aldrich). Immunoreactivity was detected by incubation with horseradish peroxidase-conjugated goat anti-rat IgG, anti-rabbit IgG, or anti-mouse IgG antibodies (Santa Cruz Biotechnology, Insight Biotechnology, Middlesex, UK) and an enhanced chemiluminescence kit (Millipore, Watford, UK), with subsequent digitization using an Image Reader LAS-1000 (Fujifilm, Tokyo, Japan). For quantification of the data, the images were further analyzed on the same instrument using 2D Densitometry Aida Image Analyzer software (Fujifilm). Mann-Whitney tests were used to determine statistical significance of differences in the median values of optical density of the signals corresponding to proteins of interest in CLL samples between UM-CLL and M-CLL cases.

Transmigration Assay and CCR7 Expression—Transmigration assays were carried out as described previously (29), but with the following modifications. Briefly, 5×10^5 CLL cells were added to the inserts of Transwell plates (5 μm pore size;Corning B.V., Amsterdam, The Netherlands). The CCL21 (CC chemokine ligand 21; 1 μg/ml; R&D Systems Europe, Oxford, UK) was then added to the bottom wells. The cells were incubated for 4 h at 37 °C with 5% CO_2. After incubation, the transmigrated cells from three technical replicates were counted, and the migration index was calculated (migration index = number of cells migrating in the presence of
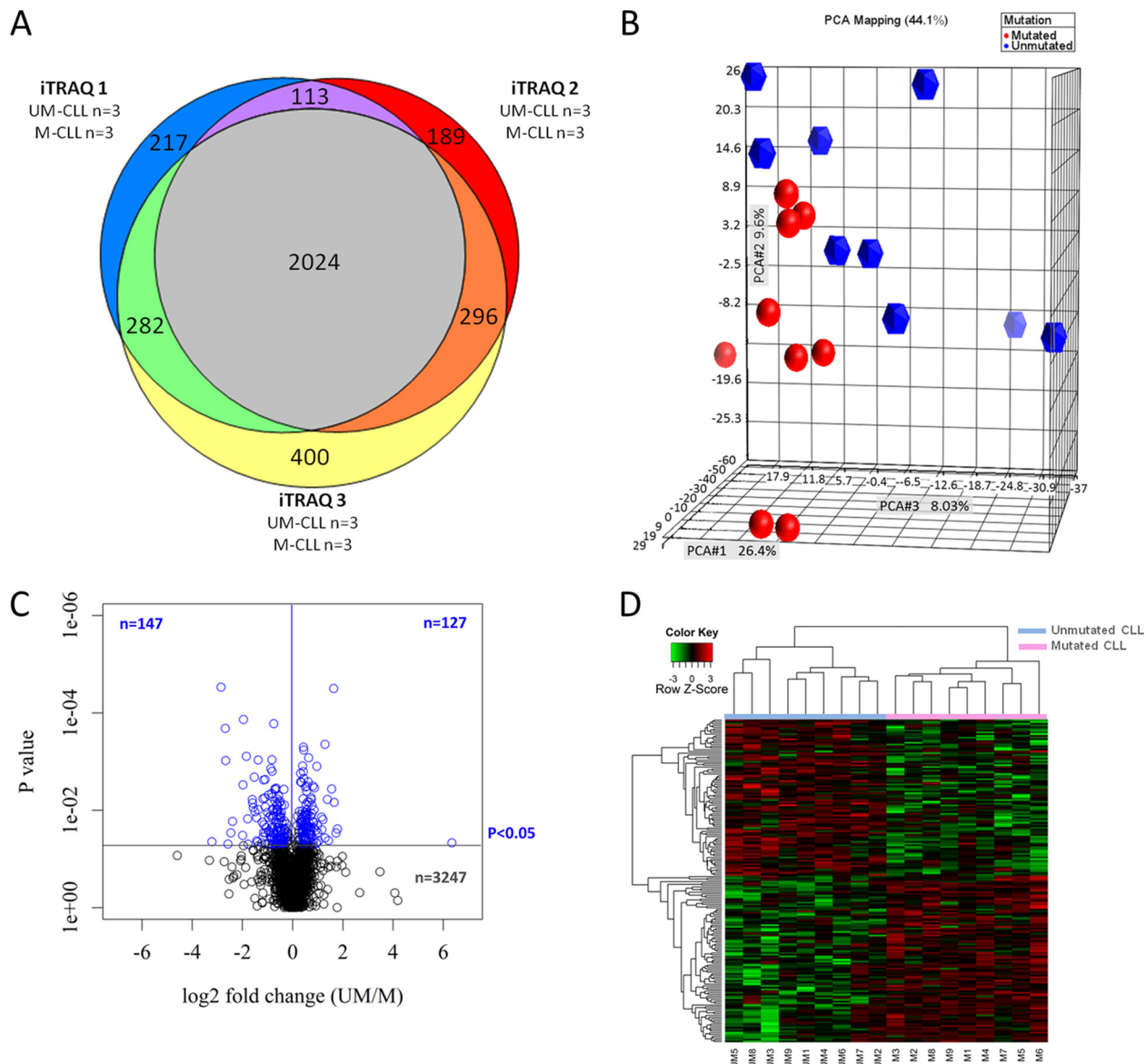
FIG. 1. **Bioinformatic analysis of proteins identified by iTRAQ-MS.** *A*, Venn diagram showing the number of proteins reproducibly identified between the three separate iTRAQ-MS experiments. In total, 3521 proteins were identified, 2024 of which were identified in all three experiments, and 2715 proteins were identified in two or more experiments. *B*, PCA showing the separation of UM-CLL and M-CLL samples based on relative protein levels. *C*, volcano plot of the entire protein data set obtained by iTRAQ-based MS showing differences in protein expression between M-CLL and UM-CLL according to magnitude and *p* value (*t* test). Protein expression was remarkably similar in the two CLL subsets, with 92% (*n* = 3247) of identified proteins sharing similar levels of expression across the sample cohort ($p > 0.05$). However, >270 proteins were differentially expressed between the two CLL subsets, giving a *p* value of <0.05, with 147 proteins being expressed at lower levels and 127 proteins expressed at higher levels in UM-CLL compared with M-CLL. *D*, heat map showing levels of differentially expressed proteins for which relative quantitative values were obtained for all 18 CLL cases (*n* = 186). Hierarchical clustering of CLL cases based on the relative expression of these proteins generated two clusters comprising the nine cases of UM-CLL and the nine cases of M-CLL, respectively.

chemokine divided by number of cells migrating in the absence of chemokine). The expression of the CCL21 receptor (CCR7) in CLL cells was measured by FACS (Becton Dickinson, Oxford, UK).

RESULTS

Quantitative Proteomic Analysis Separates CLL Samples Based on IGHV Mutational Status—To generate quantitative information on the whole proteome of CLL cells, mononuclear cells from nine M-CLL and nine UM-CLL samples containing >90% CLL cells were subjected to iTRAQ-based MS (Table 1). The two groups were well balanced in other respects, including age at diagnosis (median of 67 *versus* 70 years), prior therapy (37% *versus* 22%), and adverse chromosomal abnormalities (22% *versus* 22%), although fewer M-CLL than UM-CLL patients were male (33% *versus* 67%).

TABLE II

Chemotaxis, cell adhesion, and cytoskeletal remodeling pathway maps enriched by proteins found to be differentially expressed in M-CLL versus UM-CLL

Enriched pathways	p	FDR	No. of differentially expressed proteins in pathway	Total proteins in pathway
1. Cytoskeleton remodeling_Regulation of actin cytoskeleton by Rho GTPases	<0.001	0.000	7	23
2. Chemotaxis_Inhibitory action of lipoxins on IL-8- and leukotriene B4-induced neutrophil migration	<0.001	0.000	8	51
3. Inhibitory action of lipoxins on neutrophil migration	<0.001	0.000	8	57
4. Cell adhesion_Chemokines and adhesion	<0.001	0.000	10	100
5. Cell adhesion_IL-8-dependent cell migration and adhesion	<0.001	0.000	6	33
6. Chemotaxis_Leukocyte chemotaxis	<0.001	0.000	8	75
7. Immune response_Immunological synapse formation	<0.001	0.001	7	59
8. Cell adhesion_Histamine H1 receptor signaling in interruption of cell barrier integrity	<0.001	0.001	6	45
9. Cytoskeleton remodeling_Integrin outside-in signaling	<0.001	0.002	6	49
10. Cytoskeleton remodeling_Cytoskeleton remodeling	<0.001	0.002	8	102
11. CCR4-dependent immune cell chemotaxis in asthma and atopic dermatitis	<0.001	0.002	5	34
12. Development_S1PR1 signaling via β-arrestin	<0.001	0.002	5	34
13. Chemotaxis_CCR4-induced chemotaxis of immune cells	<0.001	0.002	5	34
14. Mechanism of action of CCR4 antagonists in asthma and atopic dermatitis (Variant 1)	<0.001	0.002	5	34
15. Immune response_CXCR4 signaling via second messenger	<0.001	0.002	5	34
16. Chemotaxis_C5a-induced chemotaxis	<0.001	0.005	5	43
17. Immune response_MIF-induced cell adhesion, migration and angiogenesis	<0.001	0.006	5	46
18. Chemotaxis_Lipoxin inhibitory action on fMLP-induced neutrophil chemotaxis	<0.001	0.006	5	46
19. Development_S1PR2 and S1PR3 in cell proliferation and differentiation	<0.001	0.006	4	26
20. Development_Thromboxane A2 pathway signaling	0.001	0.007	5	49
21. Cytoskeleton remodeling_TGF, Wnt, and cytoskeletal remodeling	0.001	0.010	7	111
22. Immune response_CCL2 signaling	0.001	0.010	5	54
23. Cell adhesion_Integrin inside-out signaling	0.001	0.011	5	56
24. Chemotaxis_CXCR4 signaling pathway	0.001	0.012	4	34
25. Development_c-Kit ligand signaling pathway during hemopoiesis	0.001	0.014	5	61
26. Cell adhesion_Role of tetraspanins in integrin-mediated cell adhesion	0.002	0.015	4	37
27. Cytoskeleton remodeling_α_{1A}-Adrenergic receptor-dependent inhibition of PI3K	0.002	0.019	3	19
28. Cytoskeleton remodeling_Role of PKA in cytoskeleton reorganization	0.002	0.019	4	40
29. Development_S1PR3 signaling pathway	0.003	0.023	4	43
30. Chemotaxis_CCL2-induced chemotaxis	0.007	0.042	4	56
31. Muscle contraction_S1PR2-mediated smooth muscle contraction	0.008	0.044	3	30
32. Cytoskeleton remodeling_RalA regulation pathway	0.008	0.044	3	30
33. Cytoskeleton remodeling_Reverse signaling by ephrin B	0.008	0.046	3	31
34. Cell adhesion_α4 integrins in cell migration and adhesion	0.011	0.057	3	34
35. G-protein signaling_S1PR2 signaling	0.012	0.059	3	35
36. Cell adhesion_Tight junctions	0.013	0.062	3	36
37. Development_S1PR1 signaling pathway	0.022	0.088	3	44
38. Development_S1PR4 signaling pathway	0.036	0.122	2	22
39. Immune response_IL-33 signaling pathway	0.043	0.134	3	57
40. Immune response_IL-18 signaling	0.048	0.144	3	60
41. Immune response_IL-17 signaling pathways	0.048	0.144	3	60
42. Cell adhesion_Cadherin-mediated cell adhesion	0.049	0.144	2	26
43. Development_Cross-talk between VEGF and angiopoietin 1 signaling pathways	0.049	0.144	2	26

FDR, false discovery rate; MIF, migration inhibitory factor; fMLP, formylmethionylleucylphenylalanine.

A total of 3521 proteins were identified within a 1% global false discovery rate and with a high confidence of correct peptide sequence assignment (Fig. 1*A* and the full list of proteins provided in the supplemental data). Of these, 2024 proteins were identified in all three separate iTRAQ-MS experiments (Fig. 1*A*). To determine whether protein expression was similar between UM-CLL and M-CLL samples, we subjected the data to PCA. As shown in Fig. 1*B*, PCA showed a distinction between UM-CLL and M-CLL samples based on protein expression.

A two-tailed t test was used to determine the statistical significance of differences in protein expression between UM-CLL and M-CLL samples. As shown in Fig. 1*C*, protein expression was largely comparable between the two CLL subsets, with 92% of proteins sharing similar levels of expression across the sample cohort. However, we found 274 proteins that were differentially expressed in UM-CLL and M-CLL samples ($p < 0.05$) (supplemental Table S2). Among them, 127 proteins were expressed at higher levels and 147 proteins at lower levels in UM-CLL samples compared with M-CLL counterparts (Fig. 1*C*). Relative quantification of 186 of 274 differentially expressed proteins was obtained across all 18 samples. As shown in Fig. 1*D*, hierarchical clustering of CLL samples based on the expression of these 186 differentially

TABLE III

39 individual proteins differentially expressed in M-CLL versus UM-CLL (p < 0.05) that are involved in chemotaxis, cell adhesion, and cytoskeletal remodeling pathways

Swiss-Prot accession No.	Gene	Protein name	Fold change (UM/M)	p
P68032	Actin cytoskeletal	Actin, α cardiac muscle 1[a]	−1.5	0.011
P63261	Actin cytoskeletal	Actin, cytoplasmic 2	−2.7	0.014
O15143	Arp2/3	Actin-related protein 2/3 complex subunit 1B	−1.4	0.038
O15144	Arp2/3	Actin-related protein 2/3 complex subunit 2	−1.8	0.001
O15145	Arp2/3	Actin-related protein 2/3 complex subunit 3	−1.6	0.014
P61158	Arp2/3	Actin-related protein 3	−1.6	0.031
P62330	ARF6	ADP-ribosylation factor 6	−1.8	0.013
P35611	Adducin 1 (α)	-αAdducin	−1.6	0.004
P63010	Actin cytoskeletal	AP-2 complex subunit β	−1.5	0.010
Q96CW1	AP complex 2 medium (μ) chain	AP-2 complex subunit μ	2.2	0.014
P16070	CD44	CD44 antigen	1.4	0.012
O43639	GRB4/NCK2	Cytoplasmic protein NCK2[a]	−1.3	0.045
Q92608	DOCK2	Dedicator of cytokinesis protein 2	−1.8	0.037
Q02750	MEK1/2	Dual specificity mitogen-activated protein kinase kinase 1	−1.4	0.007
P50570	Dynamin-2	Dynamin-2	−1.3	0.048
P02675	Fibrinogen	Fibrinogen β chain	−6.0	0.049
P02679	Fibrinogen γ	Fibrinogen γ chain	−9.3	0.044
P21333	Filamin	Filamin-A	−3.0	0.006
P04899	G protein α_i family	Guanine nucleotide-binding protein G_i subunit α-2	−1.6	0.006
P20036	MHC class II	HLA class II histocompatibility antigen, DP α1 chain	2.0	0.020
O14920	IKK-β	Inhibitor of nuclear factor κB kinase subunit β	−1.3	0.017
P20701	αLα integrin	Integrin αL	−2.1	0.023
P11215	αMβ integrin	Integrin αM	−2.6	0.010
P05107	ITGB2/βL integrin	Integrin β2	−2.3	0.046
Q9UJU2	Tcf/LEF-1	Lymphoid enhancer-binding factor 1	1.2	0.019
P49137	MAPKAP	MAPK-activated protein kinase 2[a]	−1.4	0.043
P60660	MELC/myosin	Myosin light polypeptide 6	−1.8	0.023
P24844	MRLC/myosin	Myosin regulatory light polypeptide 9	−5.5	0.029
P35579	Myosin	Myosin-9	−2.9	0.002
Q00653	NF-κB	Nuclear factor NF-κB p100 subunit	−1.3	0.035
Q14289	FAK2/Pyk2	Protein-tyrosine kinase 2β	−1.4	0.038
Q7LDG7	CalDAG-GEFI	RAS guanyl-releasing protein 2	−2.2	0.006
P08575	CD45	Receptor-type tyrosine-protein phosphatase C	−1.7	0.009
Q92888	ARHGEF1	Rho guanine nucleotide exchange factor 1	−1.5	0.049
P51812	p90^{RSK}	Ribosomal protein S6 kinase α3	−1.5	0.006
P42229	STAT5	Signal transducer and activator of transcription 5A	−1.9	0.028
Q9Y490	Talin	Talin-1	−3.5	0.015
P07996	Thrombospondin-1	Thrombospondin-1	−5.2	0.017
P50552	VASP	Vasodilator-stimulated phosphoprotein	−1.8	0.050

All proteins were identified by two or more peptides at ≥90% confidence and were present in two or more iTRAQ experiments unless indicated otherwise.

[a] Proteins were identified by a single peptide at ≥99% confidence and were present in two or more iTRAQ experiments.

expressed proteins clearly separated cases into two distinct groups corresponding to IGHV mutational status, with no samples identified as outliers.

Verification of iTRAQ-MS Data by Western Blotting—To validate the iTRAQ-MS data, we sought to verify the differential expression of a small number of proteins by Western blotting. We selected three differentially expressed proteins as follows: TCL-1 (30, 31), MNDA (32), and LEF-1 (33). The expression of TCL-1, MNDA, and LEF-1 as measured by Western blotting varied among the 18 samples (supplemental Fig. S1*A*) and correlated with IGHV mutational status with a pattern of differential expression entirely consistent with the iTRAQ-MS data (supplemental Fig. S1*B*).

UM-CLL Cells Are Characterized by Defective Cell Migration Pathways—We next used GeneGo pathway maps from MetaCore to identify pathways enriched by the 274 proteins that were differentially expressed in the two subsets of CLL samples ($p < 0.05$). The enrichment analysis identified 169 signaling pathways ($p < 0.05$) (supplemental Table S3). Remarkably, 26 of the top 50 most significantly altered pathways were associated with cell migration/adhesion. In total, 43 cell migration/adhesion pathways (Table 2) were significantly enriched by 39 differentially expressed proteins (Table 3). As all of these 39 proteins were involved in lymphocyte entry into, transit within, or exit from the lymphoid tissues (Fig. 2) and 35 of them were expressed at significantly lower levels in UM-

FIG. 2. **Schematic diagram illustrating factors involved in lymphocyte migration into, retention within, and egress from lymph nodes.** Migration into, within, and through lymphoid tissues is a complex multistep process. The major steps are illustrated here, along with the pathways/proteins that are altered in UM-CLL *versus* M-CLL. On initial contact with the endothelium, the lymphocytes become loosely tethered (*A*). If the cell encounters chemokine presented on the endothelial cell surface, it then becomes firmly adherent in a process involving integrin activation and chemokine signaling (*B*). The cell then crawls along the endothelium until it reaches an intercellular junction, where it undergoes diapedesis in response to chemokine (*C*); this process also requires integrin activation. Once within the lymphoid tissue (*D*), two different mechanisms mediate the adherence of CLL cells within the tissues; these involve $\alpha 4\beta 1$ and CD44 binding to their respective ligands, fibronectin and hyaluronan. Adhesion mediated by both substrata is influenced by chemokine signaling. The final step of transit though the lymph node is egress (*E*), a process that is entirely dependent on S1PR1 and is independent of integrins.
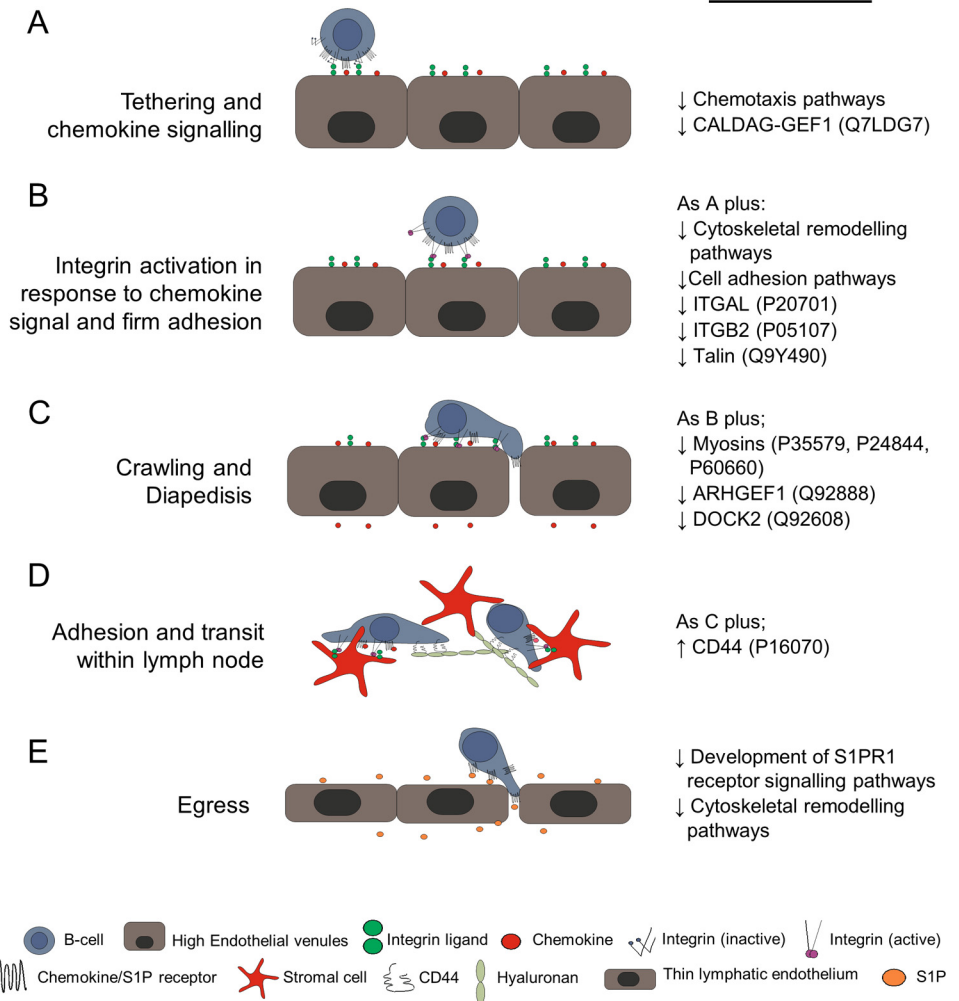
CLL samples, these results suggest that UM-CLL cells have reduced migratory properties compared with their M-CLL counterparts.

The lymphocyte chemotaxis pathway, which is essential for migration into and transit within lymphoid tissues (34), was significantly altered ($p < 0.001$) in UM-CLL cells. Of particular note, eight of the nine differentially expressed proteins in this pathway were expressed at significantly lower levels in UM-CLL samples (Fig. 3). These underexpressed proteins included the Rap (Ras-related protein) activator CalDAG-GEFI (RAS guanyl-releasing protein 2; Q7LDG7), which is involved in integrin activation (35, 36); both chains of the $\alpha L\beta 2$ integrin (P20701 and P05107), which is required for the migration of lymphocytes into lymph nodes; and talin (Q9Y490), which is important in maintaining the high-affinity binding state of $\alpha L\beta 2$ (37). Collectively, these observations strongly suggest that UM-CLL is associated with impaired Rap1-dependent $\alpha L\beta 2$-mediated migration.

We also found that CD44 (P16070), which facilitates the adhesion of CLL cells within the lymph node microenvironment (38), was expressed at significantly higher levels in UM-CLL cells, whereas two proteins that regulate S1PR1 (sphingosine 1-phosphate receptor 1) signaling, dynamin-2 (P50570) and G-protein α_i (P04899) (39, 40), were expressed at significantly lower levels. Because egress of lymphocytes from lymph nodes is absolutely dependent on S1PR1 (41), these findings suggest that the latter process is also dysfunctional in UM-CLL. In keeping with the GeneGo MetaCore pathway analysis, PANTHER analysis indicated that many of the proteins that were expressed at reduced levels in UM-CLL cells are involved in cytoskeletal remodeling (supplemental Fig. S2, *A* and *B*).

UM-CLL Cells Retain Their Ability to Migrate toward CCL21—The proteomic data suggest that UM-CLL cells have migration defects that affect both lymph node entry and exit. To formulate a hypothesis that could be validated at the clinical level, we examined one of the key steps involved in the entry
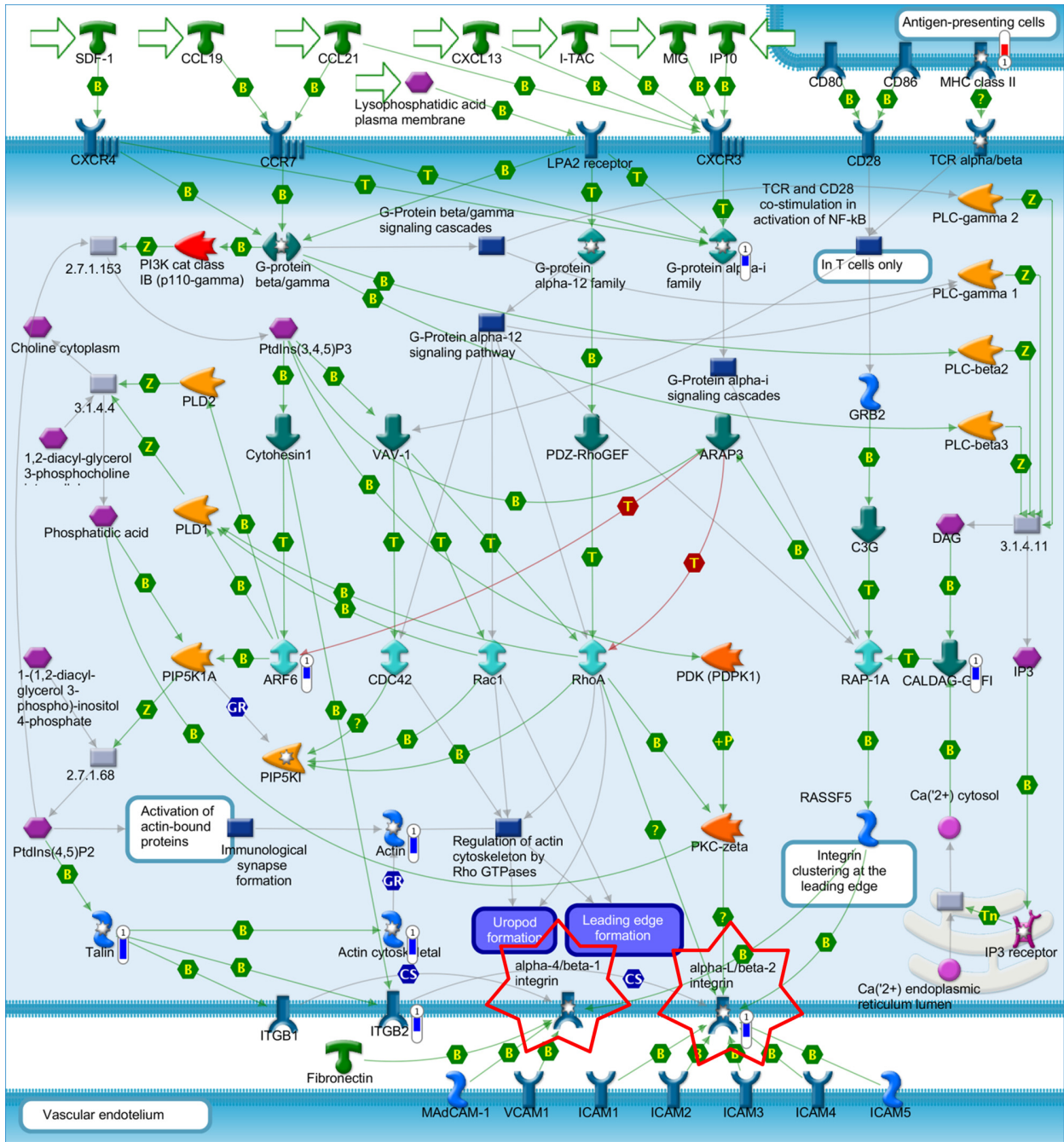
FIG. 3. **Enrichment of leukocyte chemotaxis pathway by proteins found to be differentially expressed in M-CLL *versus* UM-CLL.** One of the migration pathways most enriched by the GeneGo MetaCore pathway maps using proteins differentially expressed between UM-CLL and M-CLL was the leukocyte chemotaxis pathway ($p < 0.001$). This pathway directs leukocyte movement to lymphatic organs and also allows

of CLL cells into lymph nodes, namely, migration toward CCL21. To ascertain the functional integrity of this aspect of lymph node entry in light of our published observations that integrin activation on CLL cells is defective (29, 42, 43), CLL cells were examined for their ability to migrate in the absence of adhesion using Transwell assays. Although the UM-CLL cells tended to migrate less than the M-CLL cells, no significant differences were observed ($p = 0.713$) (supplemental Fig. S3). These data therefore support the notion that UM-CLL cells at least partly retain their ability to migrate toward CCL21 and are therefore able to enter the lymph node environment.

Patients with UM-CLL Have More Lymphadenopathy than Those with M-CLL—On the basis of our proteomic and functional data, we hypothesized that UM-CLL cells are retained in lymph nodes due to a global defect in migration coupled with impaired S1PR1-mediated egress and increased adhesion to hyaluronan within the tissue via CD44. To test this hypothesis, we examined the clinical records of patients with M-CLL ($n = 78$) and UM-CLL ($n = 42$) for documentation of lymph node enlargement. To be able to analyze lymphadenopathy independently of overall tumor burden, cases of CLL used for this comparison were selected to have similar levels of blood involvement; this was achieved by setting an upper limit for the blood leukocyte count of 130×10^9/liter. In keeping with our hypothesis, twice as many patients with UM-CLL compared with M-CLL had documented lymphadenopathy (50% *versus* 24%; $p < 0.01$) (Table 4). As expected, there was no significant difference in the leukocyte count between the two groups selected for this comparison (medians of 37×10^9/liter and 28×10^9/liter, respectively; $p > 0.05$). This indicates that the increased lymphadenopathy observed in UM-CLL is not simply a nonspecific manifestation of increased tumor burden but instead reflects the selective retention of UM-CLL cells in lymph nodes.

Other Pathways Enriched by Differentially Expressed Proteins—Although the most striking difference between M-CLL and UM-CLL cells identified by proteomic analysis was the defect in cell migration pathways in the IGHV-unmutated group, other differences were also observed. For example, PANTHER analysis showed that the majority of proteins that were overexpressed in UM-CLL cells are involved in nucleic acid binding and RNA splicing factor activity (supplemental Fig. S2, *C* and *D*), suggesting higher levels of transcriptional and translational activities in these cells. Furthermore, GeneGo MetaCore analysis showed that pathways that promote cell survival and proliferation in UM-CLL cells were

TABLE IV
Relationship between IGHV mutational status and lymphadenopathy in 120 CLL patients

Clinical feature	M-CLL ($n = 78$)	UM-CLL ($n = 42$)	p
Age (median), years	67	69	0.589
Gender (males/females)	44/34	20/22	0.443
Prior therapy (treated/untreated)	3/61	1/32	1.000
Leukocyte count (median), $\times 10^9$/liter	28.25	37.35	0.072
Lymphadenopathy $\geq$1.5 cm (yes/no)	19/59	21/21	0.0078

The extended cohort comprised all locally stored CLL cases for which IGHV mutational status was known, information on lymphadenopathy available, and leukocyte count $\leq$130 $\times 10^9$/liter. The statistical significance of the difference (p values) between the two groups was determined using a two-tailed Mann-Whitney U test for parametric data and Fisher's exact test for nonparametric data, respectively. All information presented relates to the time of sample collection.

significantly enriched (supplemental Table S3). These pathways included the immune response pathway involving B cell receptor signaling ($p = 0.006$) (supplemental Fig. S4), the endoplasmic reticulum stress response pathway ($p = 0.035$) (supplemental Fig. S5), and the Wnt signaling pathway ($p = 0.006$), where LEF-1, a critical transcription factor in this pathway (44), was significantly overexpressed in UM-CLL cells ($p = 0.019$ and 0.004 for iTRAQ-based MS and Western blot confirmation, respectively).

DISCUSSION

The aim of this study was to elucidate pathogenetic mechanisms responsible for the adverse clinical course of UM-CLL by comparing the proteome of M-CLL and UM-CLL cells. Using iTRAQ-MS, we analyzed the total proteome of 18 primary CLL samples and identified 3521 proteins, making this the largest proteomic study hitherto conducted in CLL. In agreement with previous mRNA profiling studies (8, 9), overall protein expression in the nine UM-CLL and nine M-CLL samples was largely comparable, with 92% of identified proteins sharing similar levels of expression. However, almost 8% of proteins were differentially expressed. This contrasts with the much lower proportion of genes ($<$1%) that were found to be differentially expressed in mRNA profiling studies (8, 9, 45). It can therefore be deduced that post-transcriptional regulation is an important determinant of gene expression in CLL and that differences in gene expression between M-CLL and UM-CLL are substantially greater at the protein than mRNA level.

---

them to migrate to sites of infection and/or inflammation via either $\alpha L\beta 2$ or $\alpha 4\beta 1$ integrins (highlighted). Within this pathway, nine proteins were found to be differentially expressed: MHC class II (P20036, $p = 0.02$), G-protein α_i family (P04899, $p = 0.006$), CalDAG-GEFI (Q7LDG7, $p = 0.006$), ARF6 (P62330, $p = 0.013$), actin (P68032, $p = 0.011$), actin cytoskeletal (P63261, $p = 0.014$), talin (Q9Y490, $p = 0.015$), ITGB2 (P05107, $p = 0.046$), and $\alpha L\beta 2$ (P20701, $p = 0.023$; P05107, $p = 0.046$). MHC class II had a higher expression in UM-CLL (fold changes represented by a *red thermometer*). However, the other eight differentially expressed proteins had a lower expression in UM-CLL (fold changes represented by *blue thermometers*) compared with M-CLL. This suggests that migration into the tissue microenvironments via the $\alpha L\beta 2$ integrin pathway may be dysfunctional in UM-CLL.

In keeping with this observation, it is noteworthy that PCA clearly separated CLL samples into two groups corresponding to IGHV mutational status.

After verifying the differential expression of three proteins (i.e., TCL-1, MNDA, and LEF-1), the iTRAQ-MS data were subjected to two different forms of computational analyses to explore the functional implications of the 274 differentially expressed proteins. Strikingly, both GeneGo MetaCore pathway analysis and PANTHER analysis of individual proteins revealed that a high proportion of differentially expressed proteins were involved in cell migration processes and that almost all of these were underexpressed in UM-CLL. It can therefore be concluded that UM-CLL cells have a global defect in migration.

With regard to specific migration pathways that are defective in UM-CLL, the results of the computational analysis may at first appear contradictory. Thus, although UM-CLL cells underexpressed proteins involved in egress from lymph nodes (dynamin-2 and G-protein α_i, which activate S1PR1), they also underexpressed proteins involved in lymph node entry ($\alpha L\beta 2$ integrin and CalDAG-GEFI, which activate $\alpha L\beta 2$ via Rap1, and talin, which stabilizes the integrin in its active conformation). UM-CLL cells also overexpressed CD44, which contributes to the retention of CLL cells in lymph nodes by mediating adhesion to hyaluronan following engagement of CD40 by CD154-expressing T cells in the lymph node microenvironment (38). The overall impact of these different pathway defects clearly depends on which are functionally most important. Pertinent to this consideration is our previous demonstration that Rap1-dependent $\alpha L\beta 2$ activation is defective in CLL but that this defect can be overcome if $\alpha 4\beta 1$ is coexpressed (43). Other groups have shown that surface $\alpha 4\beta 1$ expression is higher in UM-CLL (46). We therefore speculated that the $\alpha L\beta 2$ defect in UM-CLL cells is counteracted by their increased surface expression of $\alpha 4\beta 1$. In keeping with this idea, we found that UM-CLL cells at least partially retain their ability to migrate toward CCL21, which is required for lymph node entry (42, 47). This led us to formulate the hypothesis that in UM-CLL, defective lymph node entry is more than compensated for by enhanced retention and impaired egress, resulting in the selective accumulation of the malignant cells in lymph nodes. To test this hypothesis, we related lymph node enlargement to IGHV status in a cohort of 120 patients and observed that lymphadenopathy was twice as common in patients with UM-CLL compared with those with M-CLL. The association between UM-CLL and lymph node enlargement was not simply a reflection of increased tumor burden, as the M-CLL and UM-CLL patients used for this comparison had similar levels of blood involvement.

Retention of CLL cells in lymph nodes is likely to have profound implications for disease pathogenesis, given that the lymph node microenvironment provides crucial proliferative stimuli (48–50) and that lymph node enlargement is associated with adverse clinical outcome (51–53). In keeping with this concept, PANTHER analysis revealed that the majority of proteins that were overexpressed in UM-CLL cells had nucleic acid binding and RNA splicing factor activity. It is also of interest that UM-CLL cells displayed a pattern of protein expression indicating increased activity in B cell receptor signaling, endoplasmic reticulum stress response, and Wnt signaling pathways. These properties of UM-CLL cells could be intrinsic to their differentiation/maturation status. Alternatively, they could represent changes induced by extrinsic stimuli during their delayed passage through the lymph node microenvironment that are retained after the cells have re-entered the blood stream.

The concept that UM-CLL cells are preferentially retained in lymph nodes, where they are exposed to proliferative stimuli, suggests that therapeutic strategies that displace CLL cells from lymph nodes may be particularly effective in UM-CLL. In agreement with this prediction, clinical studies have shown that the overall response to ibrutinib, an inhibitor of Bruton tyrosine kinase that redistributes CLL cells from tissues into the blood by preventing tissue adhesion and homing (54–56), is significantly higher in patients with UM-CLL (77%) compared with those with M-CLL (33%) ($p = 0.005$) (57). Very similar findings have been observed with idelalisib (58), a selective inhibitor of the phosphoinositide 3'-kinase p110 delta isoform that mobilizes CLL cells into the blood by interfering with microenvironmental interactions (59, 60).

In conclusion, we have shown that quantitative analysis of the total proteome by iTRAQ-MS was able to separate individual CLL cases according to IGHV status and explain the more aggressive clinical behavior of UM-CLL and its particular sensitivity to treatments that induce anatomical displacement from the lymph node microenvironment. More generally, and in accordance with the ability of proteomic analysis to detect alterations in gene expression resulting from both transcriptional and post-transcriptional mechanisms (61, 62), the study illustrates the considerable potential of iTRAQ-MS coupled with a systems biology approach to elucidate pathogenetic mechanisms and indicate therapeutic strategies in cancer.

§§ To whom correspondence may be addressed: Department of Molecular and Clinical Cancer Medicine, Institute of Translational Medicine, University of Liverpool, 6th floor, Duncan Building, Daulby Street, Liverpool L69 3GA, United Kingdom. E-mail: a.r.pettitt@liverpool.ac.uk.

REFERENCES

1. Chiorazzi, N., Rai, K. R., and Ferrarini, M. (2005) Chronic lymphocytic leukemia. *N. Engl. J. Med.* **352,** 804–815
2. Zenz, T., Mertens, D., Küppers, R., Döhner, H., and Stilgenbauer, S. (2010) From pathogenesis to treatment of chronic lymphocytic leukaemia. *Nat. Rev. Cancer* **10,** 37–50
3. Zenz, T., Häbe, S., Denzel, T., Mohr, J., Winkler, D., Bühler, A., Sarno, A., Groner, S., Mertens, D., Busch, R., Hallek, M., Döhner, H., and Stilgenbauer, S. (2009) Detailed analysis of p53 pathway defects in fludarabine-refractory chronic lymphocytic leukemia (CLL): dissecting the contribution of 17p deletion, TP53 mutation, p53-p21 dysfunction, and miR34a in a prospective clinical trial. *Blood* **114,** 2589–2597
4. Damle, R. N., Wasil, T., Fais, F., Ghiotto, F., Valetto, A., Allen, S. L., Buchbinder, A., Budman, D., Dittmar, K., Kolitz, J., Lichtman, S. M., Schulman, P., Vinciguerra, V. P., Rai, K. R., Ferrarini, M., and Chiorazzi, N. (1999) Ig V gene mutation status and CD38 expression as novel prognostic indicators in chronic lymphocytic leukemia. *Blood* **94,** 1840–1847
5. Hamblin, T. J., Davis, Z., Gardiner, A., Oscier, D. G., and Stevenson, F. K. (1999) Unmutated Ig V_H genes are associated with a more aggressive form of chronic lymphocytic leukemia. *Blood* **94,** 1848–1854
6. Cramer, P., and Hallek, M. (2011) Prognostic factors in chronic lymphocytic leukemia–what do we need to know? *Nat. Rev. Clin. Oncol.* **8,** 38–47
7. Seifert, M., Sellmann, L., Bloehdorn, J., Wein, F., Stilgenbauer, S., Dürig, J., and Küppers, R. (2012) Cellular origin and pathophysiology of chronic lymphocytic leukemia. *J. Exp. Med.* **209,** 2183–2198
8. Klein, U., Tu, Y., Stolovitzky, G. A., Mattioli, M., Cattoretti, G., Husson, H., Freedman, A., Inghirami, G., Cro, L., Baldini, L., Neri, A., Califano, A., and Dalla-Favera, R. (2001) Gene expression profiling of B cell chronic lymphocytic leukemia reveals a homogeneous phenotype related to memory B cells. *J. Exp. Med.* **194,** 1625–1638
9. Rosenwald, A., Alizadeh, A. A., Widhopf, G., Simon, R., Davis, R. E., Yu, X., Yang, L., Pickeral, O. K., Rassenti, L. Z., Powell, J., Botstein, D., Byrd, J. C., Grever, M. R., Cheson, B. D., Chiorazzi, N., Wilson, W. H., Kipps, T. J., Brown, P. O., and Staudt, L. M. (2001) Relation of gene expression phenotype to immunoglobulin mutation genotype in B cell chronic lymphocytic leukemia. *J. Exp. Med.* **194,** 1639–1647
10. Lian, Z., Wang, L., Yamaga, S., Bonds, W., Beazer-Barclay, Y., Kluger, Y., Gerstein, M., Newburger, P. E., Berliner, N., and Weissman, S. M. (2001) Genomic and proteomic analysis of the myeloid differentiation program. *Blood* **98,** 513–524
11. Duncan, M. W., and Hunsucker, S. W. (2005) Proteomics as a tool for clinically relevant biomarker discovery and validation. *Exp. Biol. Med.* **230,** 808–817
12. Rabilloud, T., Chevallet, M., Luche, S., and Lelong, C. (2010) Two-dimensional gel electrophoresis in proteomics: past, present and future. *J. Proteomics* **73,** 2064–2077
13. Cochran, D. A., Evans, C. A., Blinco, D., Burthem, J., Stevenson, F. K., Gaskell, S. J., and Whetton, A. D. (2003) Proteomic analysis of chronic lymphocytic leukemia subtypes with mutated or unmutated Ig V_H genes. *Mol. Cell. Proteomics* **2,** 1331–1341
14. Scielzo, C., Ghia, P., Conti, A., Bachi, A., Guida, G., Geuna, M., Alessio, M., and Caligaris-Cappio, F. (2005) HS1 protein is differentially expressed in chronic lymphocytic leukemia patient subsets with good or poor prognoses. *J. Clin. Invest.* **115,** 1644–1650
15. Rees-Unwin, K. S., Faragher, R., Unwin, R. D., Adams, J., Brown, P. J., Buckle, A. M., Pettitt, A., Hutchinson, C. V., Johnson, S. M., Pulford, K., Banham, A. H., Whetton, A. D., Lucas, G., Mason, D. Y., and Burthem, J. (2010) Ribosome-associated nucleophosmin 1: increased expression and shuttling activity distinguishes prognostic subtypes in chronic lymphocytic leukaemia. *Br. J. Haematol.* **148,** 534–543
16. Barnidge, D. R., Jelinek, D. F., Muddiman, D. C., and Kay, N. E. (2005) Quantitative protein expression analysis of CLL B cells from mutated and unmutated IgV$_H$ subgroups using acid-cleavable isotope-coded affinity tag reagents. *J. Proteome Res.* **4,** 1310–1317
17. Alsagaby, S. A., Khanna, S., Hart, K. W., Pratt, G., Fegan, C., Pepper, C., Brewis, I. A., and Brennan, P. (2014) Proteomics-based strategies to identify proteins relevant to chronic lymphocytic leukemia. *J. Proteome Res.* **13,** 5051–5062
18. Perrot, A., Pionneau, C., Nadaud, S., Davi, F., Leblond, V., Jacob, F., Merle-Béral, H., Herbrecht, R., Béné, M. C., Gribben, J. G., Bahram, S., and Vallat, L. (2011) A unique proteomic profile on surface IgM ligation in unmutated chronic lymphocytic leukemia. *Blood* **118,** e1–e15
19. Issaq, H., and Veenstra, T. (2008) Two-dimensional polyacrylamide gel electrophoresis (2D-PAGE): advances and perspectives. *BioTechniques* **44,** 697–698, 700
20. Hallek, M., Fischer, K., Fingerle-Rowson, G., Fink, A. M., Busch, R., Mayer, J., Hensel, M., Hopfinger, G., Hess, G., von Grünhagen, U., Bergmann, M., Catalano, J., Zinzani, P. L., Caligaris-Cappio, F., Seymour, J. F., Berrebi, A., Jäger, U., Cazin, B., Trneny, M., Westermann, C., Wendtner, C. M., Eichhorst, B. F., Staib, P., Bühler, A., Winkler, D., Zenz, T., Böttcher, S., Ritgen, M., Mendila, M., Kneba, M., Döhner, H., Stilgenbauer, S., International Group of Investigators, German Chronic Lymphocytic Leukaemia Study Group (2010) Addition of rituximab to fludarabine and cyclophosphamide in patients with chronic lymphocytic leukaemia: a randomised, open-label, phase 3 trial. *Lancet* **376,** 1164–1174
21. Carter, A., Lin, K., Sherrington, P. D., Atherton, M., Pearson, K., Douglas, A., Burford, A., Brito-Babapulle, V., Matutes, E., Catovsky, D., and Pettitt, A. R. (2006) Imperfect correlation between p53 dysfunction and deletion of TP53 and ATM in chronic lymphocytic leukaemia. *Leukemia* **20,** 737–740
22. Campbell, M. J., Zelenetz, A. D., Levy, S., and Levy, R. (1992) Use of family specific leader region primers for PCR amplification of the human heavy chain variable region gene repertoire. *Mol. Immunol.* **29,** 193–203
23. Fais, F., Ghiotto, F., Hashimoto, S., Sellars, B., Valetto, A., Allen, S. L., Schulman, P., Vinciguerra, V. P., Rai, K., Rassenti, L. Z., Kipps, T. J., Dighiero, G., Schroeder, H. W., Jr., Ferrarini, M., and Chiorazzi, N. (1998) Chronic lymphocytic leukemia B cells express restricted sets of mutated and unmutated antigen receptors. *J. Clin. Invest.* **102,** 1515–1525
24. Kitteringham, N. R., Abdullah, A., Walsh, J., Randle, L., Jenkins, R. E., Sison, R., Goldring, C. E., Powell, H., Sanderson, C., Williams, S., Higgins, L., Yamamoto, M., Hayes, J., and Park, B. K. (2010) Proteomic analysis of Nrf2 deficient transgenic mice reveals cellular defence and lipid metabolism as primary Nrf2-dependent pathways in the liver. *J. Proteomics* **73,** 1612–1631
25. Shilov, I. V., Seymour, S. L., Patel, A. A., Loboda, A., Tang, W. H., Keating, S. P., Hunter, C. L., Nuwaysir, L. M., and Schaeffer, D. A. (2007) The Paragon Algorithm, a next generation search engine that uses sequence temperature values and feature probabilities to identify peptides from tandem mass spectra. *Mol. Cell. Proteomics* **6,** 1638–1655
26. Tang, W. H., Shilov, I. V., and Seymour, S. L. (2008) Nonlinear fitting method for determining local false discovery rates from decoy database searches. *J. Proteome Res.* **7,** 3661–3667
27. Vizcaíno, J. A., Deutsch, E. W., Wang, R., Csordas, A., Reisinger, F., Ríos, D., Dianes, J. A., Sun, Z., Farrah, T., Bandeira, N., Binz, P. A., Xenarios, I., Eisenacher, M., Mayer, G., Gatto, L., Campos, A., Chalkley, R. J., Kraus, H. J., Albar, J. P., Martinez-Bartolomé, S., Apweiler, R., Omenn, G. S., Martens, L., Jones, A. R., and Hermjakob, H. (2014) ProteomeXchange provides globally coordinated proteomics data submission and dissemination. *Nat. Biotechnol.* **32,** 223–226
28. RDevelopment Core Team (2005) *R: A Language and Environment for Statistical Computing,* The R Foundation for Statistical Computing, Vienna, Austria
29. Till, K. J., Spiller, D. G., Harris, R. J., Chen, H., Zuzel, M., and Cawley, J. C. (2005) CLL, but not normal, B cells are dependent on autocrine VEGF and $\alpha4\beta1$ integrin for chemokine-induced motility on and through endothelium. *Blood* **105,** 4813–4819
30. Herling, M., Patel, K. A., Khalili, J., Schlette, E., Kobayashi, R., Medeiros, L. J., and Jones, D. (2006) TCL1 shows a regulated expression pattern in chronic lymphocytic leukemia that correlates with molecular subtypes and proliferative state. *Leukemia* **20,** 280–285
31. Mansouri, M. R., Sevov, M., Aleskog, A., Jondal, M., Merup, M., Sundström, C., Osorio, L., and Rosenquist, R. (2010) IGHV3–21 gene usage is associated with high *TCL1* expression in chronic lymphocytic leukemia. *Eur J*

Haematol **84,** 109–116

32. Joshi, A. D., Hegde, G. V., Dickinson, J. D., Mittal, A. K., Lynch, J. C., Eudy, J. D., Armitage, J. O., Bierman, P. J., Bociek, R. G., Devetten, M. P., Vose, J. M., and Joshi, S. S. (2007) *ATM, CTLA4, MNDA,* and *HEM1* in high versus low CD38 expressing B-cell chronic lymphocytic leukemia. *Clin. Cancer Res.* **13,** 5295–5304

33. Erdfelder, F., Hertweck, M., Filipovich, A., Uhrmacher, S., and Kreuzer, K. A. (2010) High lymphoid enhancer-binding factor-1 expression is associated with disease progression and poor prognosis in chronic lymphocytic leukemia. *Hematol. Rep.* **2,** e3

34. Cathcart, M. K. (2009) Signal-activated phospholipase regulation of leukocyte chemotaxis. *J. Lipid Res.* **50,** (suppl.) S231–S236

35. Kawasaki, H., Springett, G. M., Toki, S., Canales, J. J., Harlan, P., Blumenstiel, J. P., Chen, E. J., Bany, I. A., Mochizuki, N., Ashbacher, A., Matsuda, M., Housman, D. E., and Graybiel, A. M. (1998) A Rap guanine nucleotide exchange factor enriched highly in the basal ganglia. *Proc. Natl. Acad. Sci. U.S.A.* **95,** 13278–13283

36. Kinashi, T., and Katagiri, K. (2004) Regulation of lymphocyte adhesion and migration by the small GTPase Rap1 and its effector molecule, RAPL. *Immunol. Lett.* **93,** 1–5

37. Calderwood, D. A. (2004) Integrin activation. *J. Cell Sci.* **117,** 657–666

38. Girbl, T., Hinterseer, E., Grössinger, E. M., Asslaber, D., Oberascher, K., Weiss, L., Hauser-Kronberger, C., Neureiter, D., Kerschbaum, H., Naor, D., Alon, R., Greil, R., and Hartmann, T. N. (2013) CD40-mediated activation of chronic lymphocytic leukemia cells promotes their CD44-dependent adhesion to hyaluronan and restricts CCL21-induced motility. *Cancer Res.* **73,** 561–570

39. Windh, R. T., Lee, M. J., Hla, T., An, S., Barr, A. J., and Manning, D. R. (1999) Differential coupling of the sphingosine 1-phosphate receptors Edg-1, Edg-3, and H218/Edg-5 to the G_i, G_q, and G_{12} families of heterotrimeric G proteins. *J. Biol. Chem.* **274,** 27351–27358

40. Rakhit, S., Pyne, S., and Pyne, N. J. (2000) The platelet-derived growth factor receptor stimulation of p42/p44 mitogen-activated protein kinase in airway smooth muscle involves a G-protein-mediated tyrosine phosphorylation of Gab1. *Mol. Pharmacol.* **58,** 413–420

41. Matloubian, M., Lo, C. G., Cinamon, G., Lesneski, M. J., Xu, Y., Brinkmann, V., Allende, M. L., Proia, R. L., and Cyster, J. G. (2004) Lymphocyte egress from thymus and peripheral lymphoid organs is dependent on S1P receptor 1. *Nature* **427,** 355–360

42. Till, K. J., Lin, K., Zuzel, M., and Cawley, J. C. (2002) The chemokine receptor CCR7 and α4 integrin are important for migration of chronic lymphocytic leukemia cells into lymph nodes. *Blood* **99,** 2977–2984

43. Till, K. J., Harris, R. J., Linford, A., Spiller, D. G., Zuzel, M., and Cawley, J. C. (2008) Cell motility in chronic lymphocytic leukemia: defective Rap1 and $\alpha L \beta$2 activation by chemokine. *Cancer Res.* **68,** 8429–8436

44. Petropoulos, K., Arseni, N., Schessl, C., Stadler, C. R., Rawat, V. P., Deshpande, A. J., Heilmeier, B., Hiddemann, W., Quintanilla-Martinez, L., Bohlander, S. K., Feuring-Buske, M., and Buske, C. (2008) A novel role for Lef-1, a central transcription mediator of Wnt signaling, in leukemogenesis. *J. Exp. Med.* **205,** 515–522

45. Haslinger, C., Schweifer, N., Stilgenbauer, S., Döhner, H., Lichter, P., Kraut, N., Stratowa, C., and Abseher, R. (2004) Microarray gene expression profiling of B-cell chronic lymphocytic leukemia subgroups defined by genomic aberrations and VH mutation status. *J. Clin. Oncol.* **22,** 3937–3949

46. Gattei, V., Bulian, P., Del Principe, M. I., Zucchetto, A., Maurillo, L., Buccisano, F., Bomben, R., Dal-Bo, M., Luciano, F., Rossi, F. M., Degan, M., Amadori, S., and Del Poeta, G. (2008) Relevance of CD49d protein expression as overall survival and progressive disease prognosticator in chronic lymphocytic leukemia. *Blood* **111,** 865–873

47. Park, E. J., Peixoto, A., Imai, Y., Goodarzi, A., Cheng, G., Carman, C. V., von Andrian, U. H., and Shimaoka, M. (2010) Distinct roles for LFA-1 affinity regulation during T-cell adhesion, diapedesis, and interstitial migration in lymph nodes. *Blood* **115,** 1572–1581

48. Smit, L. A., Hallaert, D. Y., Spijker, R., de Goeij, B., Jaspers, A., Kater, A. P., van Oers, M. H., van Noesel, C. J., and Eldering, E. (2007) Differential Noxa/Mcl-1 balance in peripheral versus lymph node chronic lymphocytic leukemia cells correlates with survival capacity. *Blood* **109,** 1660–1668

49. van Gent, R., Kater, A. P., Otto, S. A., Jaspers, A., Borghans, J. A., Vrisekoop, N., Ackermans, M. A., Ruiter, A. F., Wittebol, S., Eldering, E.,

van Oers, M. H., Tesselaar, K., Kersten, M. J., and Miedema, F. (2008) *In vivo* dynamics of stable chronic lymphocytic leukemia inversely correlate with somatic hypermutation levels and suggest no major leukemic turnover in bone marrow. *Cancer Res.* **68,** 10137–10144

50. Herishanu, Y., Pérez-Galán, P., Liu, D., Biancotto, A., Pittaluga, S., Vire, B., Gibellini, F., Njuguna, N., Lee, E., Stennett, L., Raghavachari, N., Liu, P., McCoy, J. P., Raffeld, M., Stetler-Stevenson, M., Yuan, C., Sherry, R., Arthur, D. C., Maric, I., White, T., Marti, G. E., Munson, P., Wilson, W. H., and Wiestner, A. (2011) The lymph node microenvironment promotes B-cell receptor signaling, NF-κB activation, and tumor proliferation in chronic lymphocytic leukemia. *Blood* **117,** 563–574

51. Rai, K. R., Sawitsky, A., Cronkite, E. P., Chanana, A. D., Levy, R. N., and Pasternack, B. S. (1975) Clinical staging of chronic lymphocytic leukemia. *Blood* **46,** 219–234

52. Binet, J. L., Lepoprier, M., Dighiero, G., Charron, D., D'Athis, P., Vaugier, G., Beral, H. M., Natali, J. C., Raphael, M., Nizet, B., and Follezou, J. Y. (1977) A clinical staging system for chronic lymphocytic leukemia: prognostic significance. *Cancer* **40,** 855–864

53. Swerdlow, S. H., Campo, E., Harris, N. L., Jaffe, E. S., Pileri, S. A., Stein, H., Thiele, J., and W, V. J. (2008) *WHO Classification of Tumours of Haematopoietic and Lymphoid Tissues,* IARC Press, Lyon, France

54. de Rooij, M. F., Kuil, A., Geest, C. R., Eldering, E., Chang, B. Y., Buggy, J. J., Pals, S. T., and Spaargaren, M. (2012) The clinically active BTK inhibitor PCI-32765 targets B-cell receptor- and chemokine-controlled adhesion and migration in chronic lymphocytic leukemia. *Blood* **119,** 2590–2594

55. Ponader, S., Chen, S. S., Buggy, J. J., Balakrishnan, K., Gandhi, V., Wierda, W. G., Keating, M. J., O'Brien, S., Chiorazzi, N., and Burger, J. A. (2012) The Bruton tyrosine kinase inhibitor PCI-32765 thwarts chronic lymphocytic leukemia cell survival and tissue homing *in vitro* and *in vivo*. *Blood* **119,** 1182–1189

56. Advani, R. H., Buggy, J. J., Sharman, J. P., Smith, S. M., Boyd, T. E., Grant, B., Kolibaba, K. S., Furman, R. R., Rodriguez, S., Chang, B. Y., Sukbuntherng, J., Izumi, R., Hamdy, A., Hedrick, E., and Fowler, N. H. (2013) Bruton tyrosine kinase inhibitor ibrutinib (PCI-32765) has significant activity in patients with relapsed/refractory B-cell malignancies. *J. Clin. Oncol.* **31,** 88–94

57. Byrd, J. C., Furman, R. R., Coutre, S. E., Flinn, I. W., Burger, J. A., Blum, K. A., Grant, B., Sharman, J. P., Coleman, M., Wierda, W. G., Jones, J. A., Zhao, W., Heerema, N. A., Johnson, A. J., Sukbuntherng, J., Chang, B. Y., Clow, F., Hedrick, E., Buggy, J. J., James, D. F., and O'Brien, S. (2013) Targeting BTK with ibrutinib in relapsed chronic lymphocytic leukemia. *N. Engl. J. Med.* **369,** 32–42

58. Furman, R. R., Sharman, J. P., Coutre, S. E., Cheson, B. D., Pagel, J. M., Hillmen, P., Barrientos, J. C., Zelenetz, A. D., Kipps, T. J., Flinn, I., Ghia, P., Eradat, H., Ervin, T., Lamanna, N., Coiffier, B., Pettitt, A. R., Ma, S., Stilgenbauer, S., Cramer, P., Aiello, M., Johnson, D. M., Miller, L. L., Li, D., Jahn, T. M., Dansey, R. D., Hallek, M., and O'Brien, S. M. (2014) Idelalisib and rituximab in relapsed chronic lymphocytic leukemia. *N. Engl. J. Med.* **370,** 997–1007

59. Hoellenriegel, J., Meadows, S. A., Sivina, M., Wierda, W. G., Kantarjian, H., Keating, M. J., Giese, N., O'Brien, S., Yu, A., Miller, L. L., Lannutti, B. J., and Burger, J. A. (2011) The phosphoinositide 3′-kinase delta inhibitor, CAL-101, inhibits B-cell receptor signaling and chemokine networks in chronic lymphocytic leukemia. *Blood* **118,** 3603–3612

60. Fiorcari, S., Brown, W. S., McIntyre, B. W., Estrov, Z., Maffei, R., O'Brien, S., Sivina, M., Hoellenriegel, J., Wierda, W. G., Keating, M. J., Ding, W., Kay, N. E., Lannutti, B. J., Marasca, R., and Burger, J. A. (2013) The PI3-kinase delta inhibitor idelalisib (GS-1101) targets integrin-mediated adhesion of chronic lymphocytic leukemia (CLL) cell to cndothelial and marrow stromal sells. *PLoS ONE* **8,** e83830

61. Kim, M. S., Pinto, S. M., Getnet, D., Nirujogi, R. S., Manda, S. S., Chaerkady, R., Madugundu, A. K., Kelkar, D. S., Isserlin, R., Jain, S., Thomas, J. K., Muthusamy, B., Leal-Rojas, P., Kumar, P., Sahasrabuddhe, N. A., Balakrishnan, L., Advani, J., George, B., Renuse, S., Selvan, L. D., Patil, A. H., Nanjappa, V., Radhakrishnan, A., Prasad, S., Subbannayya, T., Raju, R., Kumar, M., Sreenivasamurthy, S. K., Marimuthu, A., Sathe, G. J., Chavan, S., Datta, K. K., Subbannayya, Y., Sahu, A., Yelamanchi, S. D., Jayaram, S., Rajagopalan, P., Sharma, J., Murthy, K. R., Syed, N., Goel, R., Khan, A. A., Ahmad, S., Dey, G., Mudgal, K., Chatterjee, A., Huang, T. C., Zhong, J., Wu, X., Shaw, P. G., Freed, D., Zahari, M. S.,

Mukherjee, K. K., Shankar, S., Mahadevan, A., Lam, H., Mitchell, C. J., Shankar, S. K., Satishchandra, P., Schroeder, J. T., Sirdeshmukh, R., Maitra, A., Leach, S. D., Drake, C. G., Halushka, M. K., Prasad, T. S., Hruban, R. H., Kerr, C. L., Bader, G. D., Iacobuzio-Donahue, C. A., Gowda, H., and Pandey, A. (2014) A draft map of the human proteome. *Nature* **509,** 575–581

62. Wilhelm, M., Schlegl, J., Hahne, H., Moghaddas Gholami, A., Lieberenz, M., Savitski, M. M., Ziegler, E., Butzmann, L., Gessulat, S., Marx, H., Mathieson, T., Lemeer, S., Schnatbaum, K., Reimer, U., Wenschuh, H., Mollenhauer, M., Slotta-Huspenina, J., Boese, J. H., Bantscheff, M., Gerstmair, A., Faerber, F., and Kuster, B. (2014) Mass-spectrometry-based draft of the human proteome. *Nature* **509,** 582–587